

Anomalous magnetization of amorphous TbFe₂, GdFe₂, and YFe₂

J. J. Rhyne

Naval Ordnance Laboratory, White Oak, Maryland 20910*
and National Bureau of Standards, Washington, D.C. 20234

J. H. Schelleng and N. C. Koon

Naval Research Laboratory, Washington, D. C. 20375

(Received 24 June 1974)

Magnetization data are presented on sputter-deposited amorphous $R\text{Fe}_2$ materials, where R represents the rare-earth elements Tb, Gd, and Y. Both the Tb and Gd compounds exhibit ferrimagnetic order with Curie temperatures approximately 40% lower than the equivalent crystalline Laves phase compounds. The 0 K saturation magnetizations of the Gd amorphous and crystalline materials are both equal to $3.9\mu_B$, while in the TbFe₂ the magnetization is significantly lower in the amorphous phase ($4.2\mu_B$ vs $5.4\mu_B$ for crystalline TbFe₂). The YFe₂ exhibits no long-range magnetic order above 3.5 K. At low temperatures large "coercive" fields appear for the TbFe₂ and increase greatly in magnitude at temperatures below 40 K, reaching 30 kG at 4 K. A possible model to explain this and other effects associated with a large random-directional local anisotropy field is presented.

I. INTRODUCTION

Bulk samples of several $R\text{-Fe}$ (R is a rare-earth element) materials of varying composition and rare-earth constituents have been prepared by direct-current rapid-sputtering techniques¹ and have been shown to be crystallographically amorphous by neutron diffraction² and x-ray scattering.³ The composition Tb_{0.33}Fe_{0.67} (TbFe₂) is the most thoroughly studied,⁴ and its structure is typical of the group with an atomic stacking based on a dense random-packed⁵ arrangement of Tb and Fe atoms. The separation distances of the atoms as determined from the radial-distribution function (Fourier transform of the scattered neutron intensity) are very close to those of Tb and Fe atom pairs in contact at their Goldschmidt or 12-fold coordination radii (1.78 Å for Tb and 1.27 Å for Fe). Similar results were found for the atomic structure of YFe₂ by neutron scattering and for the highly neutron absorbing GdFe₂ by x-ray methods.³ This is in contrast to the crystalline Laves-phase counterpart compound TbFe₂, in which the nearest-neighbor Tb-Tb atom separation is contracted to 3.2 Å.

Magnetization data are presented here for the amorphous compositions TbFe₂, GdFe₂, and YFe₂. In their amorphous form the Tb and Gd materials exhibit long-range magnetic order, but with Curie temperatures significantly reduced from the crystalline compounds. The amorphous YFe₂ exhibits only strong short-range magnetic ordering.

This series was chosen to represent the extremes of large local crystal-field interactions in the case of Tb and negligible local anisotropy for the S-state ion Gd. The Y represents a nonmagnetic "pseudo-rare-earth" substitution to provide information on the Fe-Fe exchange interaction.

It is noted that the crystal-field anisotropy ef-

fects to be discussed relative to amorphous TbFe₂ differ from conventional magnetocrystalline anisotropy, and in particular do not give rise to any bulk preferred or "easy" magnetic direction. Conceptually, as suggested from earlier results,² the local anisotropy interaction arises from the Coulombic interaction of the highly nonspherical Tb 4*f* charge distribution with the electric field produced by the neighboring ions. In the amorphous disordered case this field is of unknown and spatially varying symmetry and gives rise to a distribution of local magnetic easy axes distributed over all directions of space.

The local anisotropy energy can be expressed⁶ in terms of a crystal-field potential A_l^m , 4*f*-electron effective radii $\langle r_{4f}^l \rangle$, and spherical harmonics of the electronic coordinates $Y_l^m(\theta, \phi)$ as

$$V(r, \theta) = \sum_l \sum_{m=-l}^l A_l^m \langle r_{4f}^l Y_l^m(\theta, \phi) \rangle \quad \text{for } l = \leq 6 \text{ and even,}$$

where now the crystal-field potential A_l^m is calculated for a random-close-packed neighboring-ion configuration. As shown by Harris, Plischke, and Zuckermann⁶ the magnitude of the resulting crystal-field potential is surprisingly uniform and exhibits only a 2% rms deviation over the material in spite of the random spatial distribution of minimum energy directions. The crystal-field term with $l=2$, forbidden in cubic symmetry, is allowed here by the effective lowering of the symmetry in the amorphous structure and is the dominant energy. The direction of a given spin or group of spins is then determined by the minimum free energy, consisting of the local anisotropy plus the spatially varying exchange energies. The bulk average is then a material in which macroscopically all directions are equally hard magnetic di-

rections and energy is required to align the rare-earth spins along any single magnetization direction.

II. MAGNETIZATION OF TbFe_2

Magnetic-moment measurements were made on a 0.11-g specimen of amorphous TbFe_2 using a vibrating-sample magnetometer. The sample was part of one used earlier for the structure studies (Refs. 2 and 4, which also present some preliminary magnetization data). No variation in physical properties has been observed between different samples of this material.

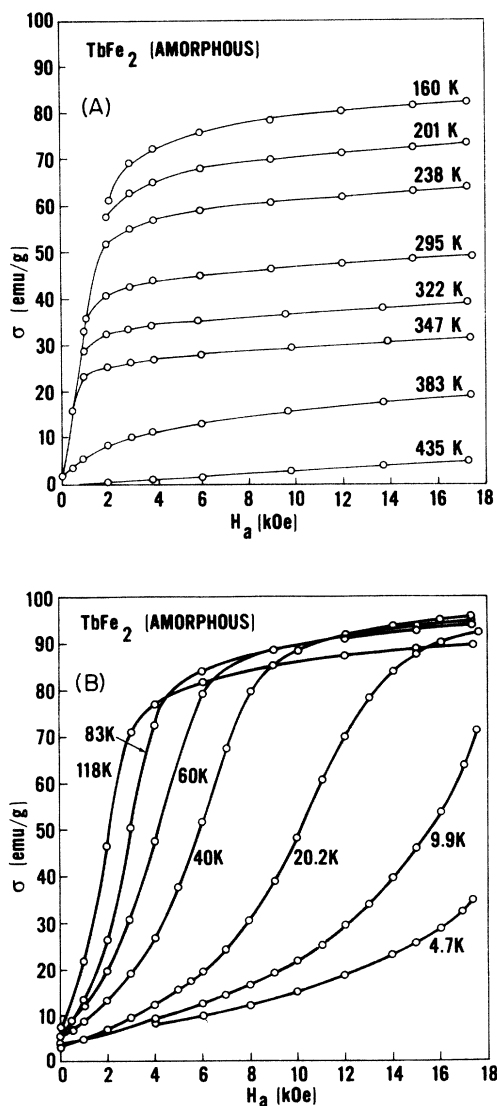


FIG. 1. (a) Magnetization isotherms for amorphous TbFe_2 above 120 K. H_a is the applied magnetic field. (b) Isotherms below 120 K showing the development of the anomalous "coercive"-force-type spin transition.

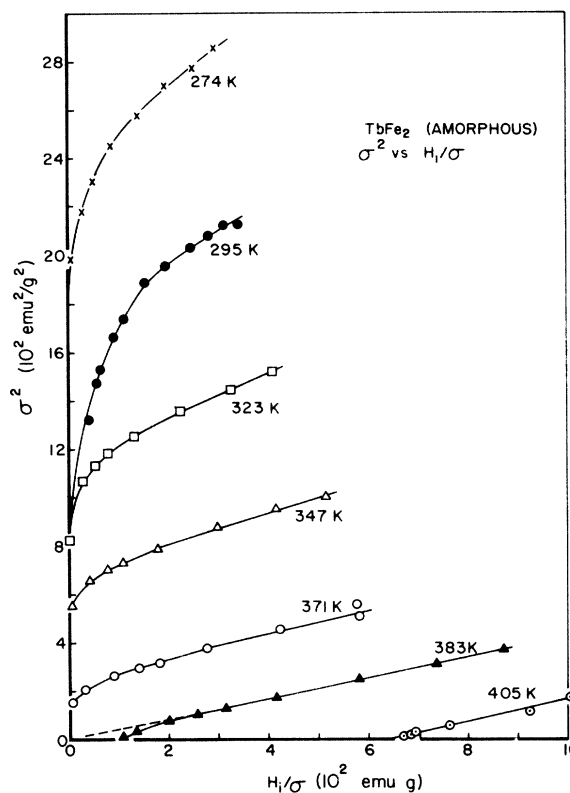


FIG. 2. Plot of σ^2 vs H_i/σ , where H_i is the applied field corrected for demagnetization effects. The effect of the nearly constant high-field susceptibility is seen in the increasing curvature at low temperatures.

Magnetization data as a function of applied field are shown in Fig. 1(a) from 435 (above the bulk Curie temperature) down to 160 K. Below about 150 K an anomalous "coercive-field"-type behavior develops in the magnetization isotherms, Fig. 1(b), and is discussed in Sec. III. The data of Fig. 1(a) indicate conventional ferromagnetic behavior except for the relatively large high-field susceptibility above technical saturation. This response suggests a somewhat loosely coupled spin system, one in which some Tb spins are not fully aligned in zero field due to the random anisotropy field brought about by the amorphous structural disorder. The magnitude of the high-field susceptibility is essentially independent of temperature, which may reflect the competing effects of increased anisotropy and increasingly more effective exchange coupling as temperature decreases. It is noted that the large susceptibility is absent for the S-state-ion material GdFe_2 discussed in Sec. IV. The effect of the high-field susceptibility of TbFe_2 is also reflected in the "Arrott" plot of σ^2 vs H/σ shown in Fig. 2, which indicates a Curie temperature close to the 383-K isotherm.

This plot is based on an expansion of the free energy of the form $F = MH + aM^2 + bM^4$, which is not a complete description for the amorphous TbFe_2 including random anisotropy as evidenced by the curvature in Fig. 2.

The spontaneous moment obtained by extrapolation of the magnetization curves back to the demagnetizing field is plotted in Fig. 3 and yields a somewhat higher Curie temperature of 409 K—a difference not considered surprising in view of the rather smeared-out character of the phase transition⁷ as observed in the critical scattering of neutrons. The dotted curve in Fig. 3 indicates the low- T region in which a reliable extrapolation could not be made due to the anomalous magnetization curves. The resulting 0-K intercept corresponds to $4.2\mu_B$ per formula unit, which is significantly lower than the $5.4\mu_B$ of the Laves-phase compound obtained by neutron diffraction⁸ and also shown in Fig. 3, or the $4.6\mu_B$ expected using an antiparallel combination of the moments of elemental Tb ($\mu = 9\mu_B$) and Fe. The reduction of the iron moment from $2.2\mu_B$ to $1.7\mu_B$ in the Laves compounds is ascribed to charge transfer⁹ from the Tb to the Fe d band, which also allows for the observed 11% contraction of the Tb-Tb nearest-neighbor separation distance below that of their metallic radii.

The amorphous magnetization results imply that the ferromagnetic Fe-Fe and antiferromagnetic Fe-Tb exchange couplings of the Laves phase are maintained, but leave open the question of the iron-moment suppression by band effects. It is in fact noted that the significant spatial contraction of the R - R pair separation distances is absent in the

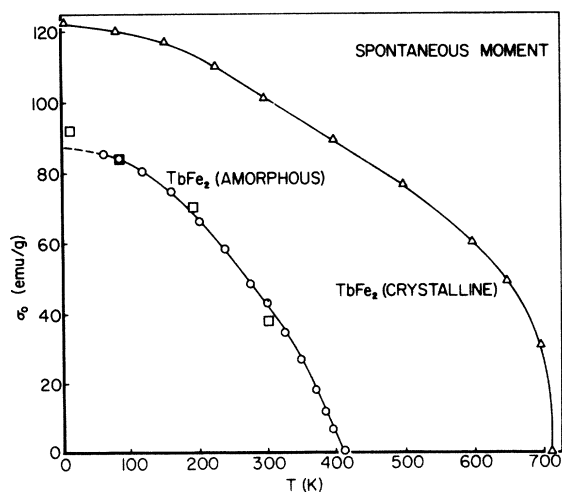


FIG. 3. Spontaneous moment for amorphous and crystalline TbFe_2 as a function of temperature. The square symbols are results from neutron diffraction (see Ref. 4).

amorphous material, but that based on the amorphous GdFe_2 results (Sec. IV) the iron moment is $1.55\mu_B$, consistent with the Laves-phase moment. This may imply that the relationship between charge-transfer effects on the itinerant Fe moment and the observed interatomic separation distances may be more complex than previously described.

The rare-earth moment is unaffected by band-structure effects, but may be effectively suppressed in a manner consistent with the observed TbFe_2 high-field susceptibility, by incomplete or noncollinear spin alignment between the Tb and Fe spins due to the local anisotropy fluctuations⁶ and/or spatial fluctuations in exchange fields¹⁰ arising from the structural disorder, both of which can also contribute⁶ to the large 45% reduction in Curie temperature shown in Fig. 3. The Curie-temperature point of the crystalline phase is from Burzo.¹¹ It is noted that the maximum moment achieved at 60 kOe and 3.5 K (see Sec. III) is $4.7\mu_B$, suggesting that the full Laves-phase moment would again be recovered in fields large enough to overcome the Tb local anisotropy and produce a uniform collinear spin alignment.

Above the ordering temperature the susceptibility of the amorphous TbFe_2 is somewhat field dependent up to the highest temperature measured (482 K) and the data do not follow a Curie-Weiss temperature dependence. Both of these results indicate a degree of short-range order persisting to temperatures more than 20% higher than the Curie point.

III. LOW-TEMPERATURE CRYSTAL-FIELD EFFECTS

The low- T magnetization curves of Fig. 1(b) show the development of large "coercive-like" fields which increase dramatically at low temperatures and reach 30 kOe at 4.2 K.¹² The sample was annealed to above 250 K between each magnetization in Fig. 1(b) to remove the remanent magnetization. High-field hysteresis loops as in Fig. 4 were also taken without annealing to determine the temperature dependence of the coercive or spin-reversal field. This field corresponded closely to the field required to achieve technical saturation in the "virgin" curves of Fig. 1(b) which do not exhibit the abrupt spin-flip field found in the hysteresis-loop results. The general features of the 4.9-K hysteresis loop are characteristic also of those at higher temperature, while below this temperature a "squaring-off" of the loop was observed as in the 1.5-K data shown. This effect and the associated slight decrease in transition field are believed to arise from local magnetothermal heating of the sample during the spin-reversal process at low temperatures where the specific heat is vanishingly small. The temperature dependence of the spin-flip field is plotted in Fig. 5. Also shown

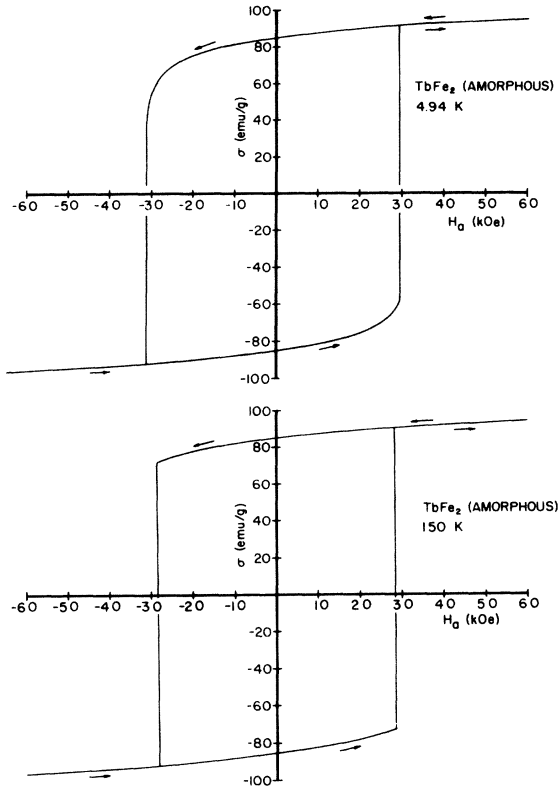


FIG. 4. Hysteresis loops at low temperatures showing the giant coercive fields in TbFe_2 . The squaring off of the 1.5-K curve is ascribed to a magnetothermal effect (see text).

is the temperature dependence of the remanent magnetization determined as a fraction of the maximum measured magnetization at a particular temperature. The transition fields decreased somewhat with increased magnetic field sweep rates at low temperature as shown by the scatter below 3 K, which is also ascribed to the magnetothermal heating process mentioned above.

The occurrence of the anomalously large spin-flip fields and their extreme temperature dependence is quite unconventional, especially considering that much of the increased effect takes place below the temperature ($40 \text{ K} = 0.1 T_c$) at which the magnetization and anisotropy energies are saturated. The steep rise with decreasing temperature suggests a form of a thermal activation process, and leads to the following postulated model for a noncollective spin transition which depends on the random distribution of rare-earth spin directions in a loosely coupled material. In this case, the angular dependence of the magnetic free energy for each spin (or a tightly coupled group of spins) will differ, depending upon the combined effects of the local anisotropy, the applied field, and the

local exchange field acting between groups. If the anisotropy energy is at least of the same order of magnitude as the applied and exchange fields, this energy distribution will have two minima and the reversal of the moment of a spin (or group of spins) will involve a discontinuous flip. Under the action of an applied field of appropriate magnitude, the flip of the spin (or group of spins) in the most favorable energy condition will occur. This would alter the local exchange field of neighboring systems and they would follow in cascade. If the thermal energy kT is comparable with the energy barrier between minima, a sharp T dependence, such as seen in Fig. 5, would result. To obtain a very crude idea of the feasibility of such an activation-energy model, one may apply the calculations for a cluster-model superparamagnet¹³ keeping in mind that the concept of weakly interacting magnetic clusters is probably not fully applicable in this material, for which all ion sites are magnetic and the magnetic order is long range. Nevertheless, using this model, if one assumes a twofold anisot-

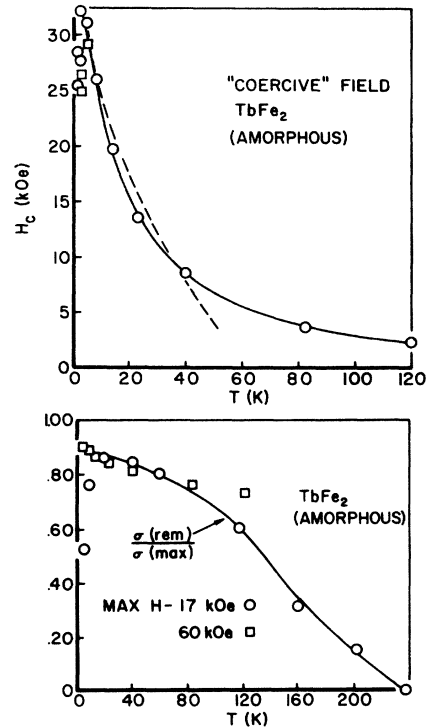


FIG. 5. (a) Temperature dependence of the coercive field obtained from hysteresis-loop measurements. The dashed line is the result of a calculated approximate temperature dependence (see text). H_c values at the lowest temperatures are affected by magnetothermal heating. (b) Temperature variation of the remanent magnetization determined as a fraction of the maximum magnetization reached at temperature T . Data were taken in both 17- and 60-kOe maximum applied fields.

ropy energy minimum in the direction of the applied field and neglects intercluster exchange, then the rate of 180° (+ to -) spin reversals becomes

$$\frac{dN_+}{dt} = -\frac{1}{\tau}N_+ + (\text{term describing inverse spin reversals}), \quad (1)$$

where N_+ is the number of spins reversing direction. Near the critical transition field then one can neglect the last (inverse-reversal) term and the time constant for the spin-flip process becomes¹³

$$\frac{1}{\tau} = \nu_0 \exp \frac{V(3K - NH)^2}{4KkT}, \quad (2)$$

where ν_0 is the natural precession frequency for spin rotation in the material. K is the $l=2$ anisotropy constant and V is the volume of the spin unit to be flipped. If one gradually increases the field, starting in the negative-moment saturated state of Fig. 4, the time constant of the spin flips gradually shortens until at the critical field it reaches the order of fractional seconds and the transition appears to take place discontinuously. In principle the transition could be induced at a lower field after a sufficient waiting time.

The assumption underlying expression (2) of a collinear applied and anisotropy field direction for all Tb spins and the neglect of intercluster exchange in amorphous TbFe is admittedly unrealistic. A properly performed direction-dependent average including exchange will have the effect of modifying the K and H in expression (2) and necessitate averaging the exponential over all rare-earth sites. Nevertheless, the result of applying expression (2) with the arbitrary choice of $\tau = 1/\nu_0 e$ sec is shown by the dashed line of Fig. 5. The values of K and V used in the fitting ($K = 1.5 \times 10^7$ erg/cm³, $V = 520 \text{ \AA}^3$) have no precise physical meaning because of the above mentioned averaging; however, the over-all functional form expressed by (2) does represent the data reasonably well from the lowest temperature to above 40 K. One may assume that with suitable modification for the amorphous structure this activation-energy spin-flip model may explain the observed rapid temperature dependence of H_c . The upper bound on the observed H_c as $T \rightarrow 0$ will be given by the appropriately averaged local anisotropy and exchange energy. If the anisotropy energy dominates the coercive-field behavior, then the maximum coercive fields for various substituted rare earths should follow the $l=2$ quadrupole-moment-operator equivalent factor¹⁴ $\alpha Y_2^0(\bar{J})$ for the particular rare-earth ion. One would thus conclude that DyFe₂ would show a similar maximum H_c and SmFe₂ would be about 40% smaller. High-field measurements at 4 K by Clark¹² have given

transition fields of 32 kOe for DyFe₂ and 21 kOe for SmFe₂, which when compared to the 30 kOe for TbFe₂ confirm reasonably well the expected anisotropy dependence.

IV. MAGNETIZATION OF AMORPHOUS GdFe₂

The absence of appreciable local single-ion anisotropy in amorphous GdFe₂ produces several significant changes in the magnetization compared to TbFe₂. The isothermal-magnetization data of Fig. 6 again are characteristic of a ferromagnet, but without the significant high-field susceptibility seen in the TbFe₂. The apparent soft coupling of some spins observed in TbFe₂ appears to be absent in the nonanisotropic GdFe₂ and confirms its local anisotropy origin. No hysteresis or measurable coercive field was observed down to 4 K. The spontaneous moment obtained from the isothermal-magnetization data is plotted in Fig. 7 and compared to the moment of crystalline GdFe₂ from Burzo.¹¹ The Curie point of 500 K is fractionally somewhat less suppressed below that of the crystalline material ($T = 795$ K) than in TbFe₂, while, in marked contrast to the terbium system, the 0-K saturation moment of amorphous GdFe₂ corresponds to that of the crystalline material. This represents the absence of local crystal-field anisotropy effects on the spin alignment and on T_c .⁶ The slight drop in moment below 40 K is reproducible but not understood. The fully saturated moment corresponds to $1.55 \mu_B$ for the Fe and the antiparallel-spin arrangement. The agreement between iron moments in both amorphous and crystalline GdFe₂ suggests a degree of Tb \rightarrow Fe charge transfer may occur also in the amorphous phase. However, as mentioned in Sec. II, the ac-

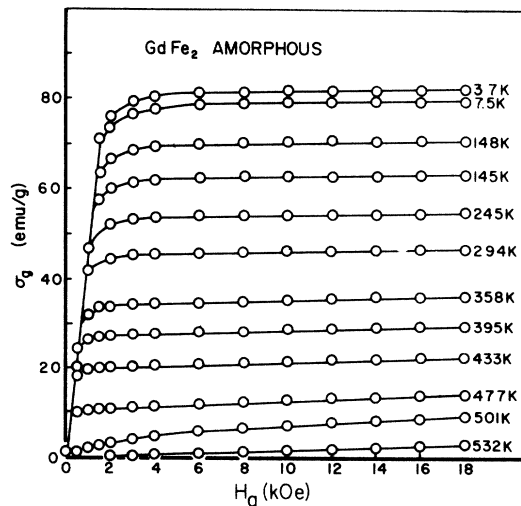


FIG. 6. Magnetization isotherms for amorphous GdFe₂.

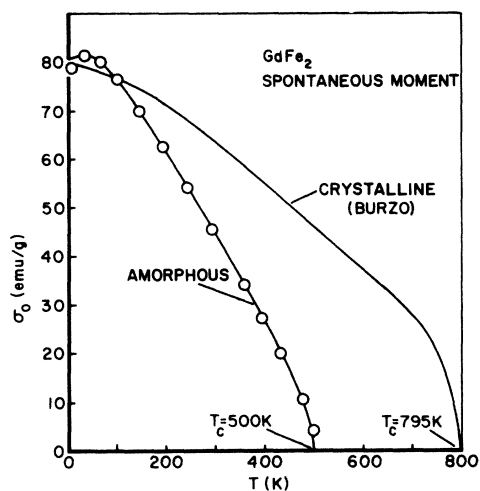


FIG. 7. Spontaneous moment for amorphous and crystalline GdFe_2 as a function of temperature.

companying large contraction of the R - R nearest-neighbor distance in the Laves phase is not found for the amorphous structures, although a small reduction was found by Cargill³ in the Gd material. The Curie temperature of amorphous GdFe_2 determined from a plot of σ^2 vs H/σ is 500 K. Plotted in this fashion the data are reasonably linear both above and considerably below T_C in contrast to the TbFe_2 . The Curie temperature of 500 K is in agreement with that found also for thin-film ($\approx 2000 \text{ \AA}$) sputtered samples.¹⁵ The data differ in some detail from a previous measurement¹⁶ on $\text{Gd}_x\text{Fe}_{1-x}$ amorphous films prepared by coevaporation onto a nitrogen-cooled substrate. Their re-

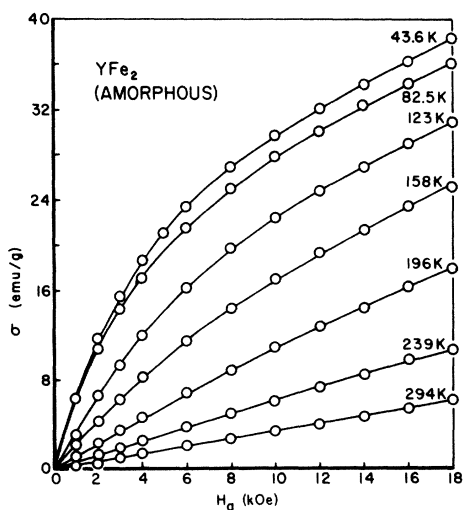


FIG. 8. Isotherms for amorphous YFe_2 illustrating behavior characteristic of only short-range ordering.

sults on $\text{Gd}_{0.32}\text{Fe}_{0.68}$ at 77 and 294 K indicated a significantly lower over-all magnetization and a lack of saturation in 8-kOe applied fields. This may indicate an increased degree of strain-induced disorder or impurity effects in the thin evaporated films.

V. NONMAGNETIC YFe_2

The substitution of nonmagnetic Y (or Lu) for a magnetic rare earth can provide a direct measure of the host (in this case Fe) sublattice magnetization and exchange energies. Under the assumption that the magnetic order and Curie temperature are primarily determined by the iron-iron exchange, then by analogy with the terbium and gadolinium amorphous rare-earth-iron systems, one would have expected YFe_2 to be magnetic with a Curie temperature near 320 K, compared to the polycrystalline value of 535 K. Anomalous, the amorphous YFe_2 exhibits only strong short-range order down to 3.5 K, the lowest temperature used, with no evidence of development of long-range ordered

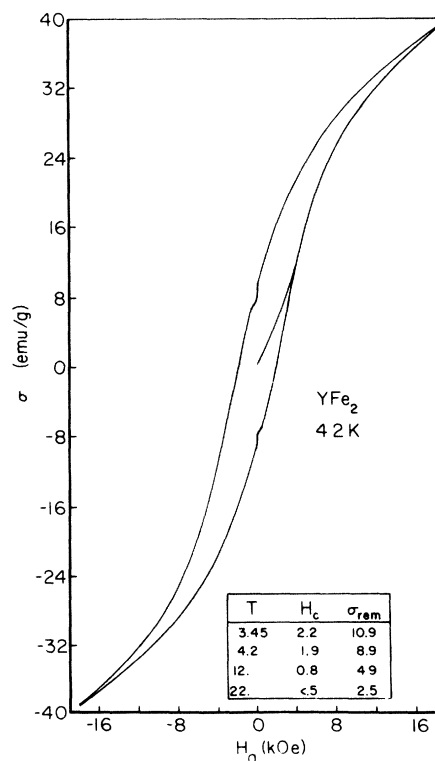


FIG. 9. Low-temperature hysteresis loop for YFe_2 indicating small-particle-type magnetic behavior. The small "blips" at 0 applied field are the time dependence of the remanent moment over a period of approximately 1 min. The insert gives representative values of the coercive field and remanent magnetization at several temperatures.

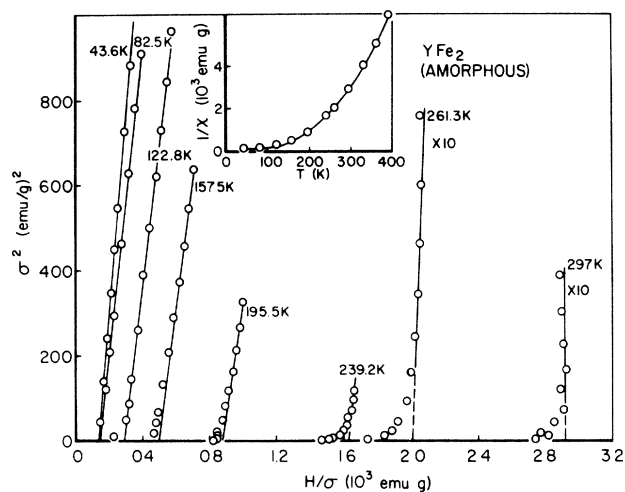


FIG. 10. Plot of σ^2 vs H_a/σ for YFe_2 . The inset displays the inverse susceptibility obtained from the H_a/σ intercept vs temperature

magnetism as shown by the isotherms of Fig. 8. The maximum moment achieved at 18 kOe corresponds to $0.7\mu_B$ per iron atom. Additional high-field magnetization measurements at 1.5 K and 60 kOe ($H/T = 40$ kOe/K sufficient to saturate a system of local free paramagnetic spins) produced a moment of $1.1\mu_B$ per iron atom still far from saturation. This suggests an itinerant-moment interpretation for the iron magnetization. At temperatures below about 50 K, a small hysteresis and remanent magnetization develops which increases at lower temperatures to 1.8 kOe and 9.4 emu/g, respectively, at 4.2 K as given in Fig. 9. The remanent magnetization is time dependent and decreases by about 10% after 1 min.

The over-all magnetic behavior of YFe_2 suggests the presence of weakly interactive small magnetic clusters. Plotting the amorphous YFe_2 data as σ^2 vs H/σ (except in the temperature range where the hysteresis exists) in Fig. 10 yields intercepts on the H/σ axis characteristic of over-all paramagnetic order. The curves depart from a straight line and curve toward the origin at low fields. The reciprocal susceptibility obtained from this plot

(Fig. 10 inset) does not show Curie-Weiss behavior. The reciprocal susceptibility also does not have the functional form $aT^2 + bT^4$ as appropriate for itinerant-moment systems above T_c , again implying the persistence of strong short-range-cluster spin ordering.

VI. CONCLUSIONS

The predominant features of the Tb, Gd, and Y systems are the existence of ferromagnetic (or ferri-magnetic) order in the first two materials and only short-range-cluster order in the YFe_2 . In addition the Tb material shows a comparatively large susceptibility below T_c and a giant "coercive-field" effect at low temperature. The data plus the form of the low-angle magnetic scattering observed in the neutron studies⁷ on $TbFe_2$ strongly suggest the existence of a magnetic coherence distance considerably greater than the atomic coherence distances (but not infinite). A possible qualitative explanation of these effects is to postulate that the exchange interaction between iron atoms is of quite short range, possibly only nearest neighbor, and that the coupling of iron to rare earths is much weaker (or absent in the case of Y) than the Fe-Fe exchange coupling. Phenomenologically then this means that the presence of the rare earth partially or fully breaks up the long-range nature of the magnetic order. This "impurity" interruption of the Fe-Fe nearest-neighbor exchange will occur along any path taken from a given iron site and an average of these path lengths may define the size of the spin "unit" which gives rise to the clusterlike behavior observed in the YFe_2 and also prescribes the spin volume necessary to account for the low-temperature behavior of the $TbFe_2$.

ACKNOWLEDGMENTS

We have benefitted from discussions with J. R. Cullen, S. J. Pickart, A. E. Clark, H. A. Alperin, S. Kirkpatrick, S. Cargill, and M. Zuckermann, all of whom have contributed to various phases of the study of the sputter-deposited rare-earth materials.

*Supported in part by the NOL Independent Research Fund, the Naval Air Systems Command, and the Office of Naval Research.

¹Disk-shaped samples approximately 2.5 cm in diameter and 1 to 3 mm thick were prepared by Battelle Northwest Laboratories under contract with the Advanced Research Projects Agency, and were furnished by R. Allen.

²J. J. Rhyne, S. J. Pickart, and H. A. Alperin, Phys. Rev. Lett. **29**, 1562 (1972); J. J. Rhyne, S. J. Pickart,

and H. A. Alperin, *Amorphous Magnetism*, edited by H. O. Hooper and A. M. DeGraaf (Plenum, New York, 1973), p. 373; and S. Pickart, J. Rhyne, H. Alperin, and H. Savage, Phys. Lett. A **47**, 73 (1974).

³G. S. Cargill, AIP Conf. Proc. **18**, 631 (1974).

⁴J. J. Rhyne, S. J. Pickart and H. A. Alperin, AIP Conf. Proc. **18**, 563 (1974).

⁵D. E. Polk, J. Non-Cryst. Solids **11**, 381 (1973).

⁶R. Harris, M. Plischke, and M. J. Zuckermann, Phys. Rev. Lett. **31**, 160 (1973); R. M. Cochrane, R. Harris,

- and M. Plischke, *J. Non-Cryst. Solids* (to be published).
- ⁷S. J. Pickart, J. J. Rhyne, and H. A. Alperin, *Phys. Rev. Lett.* 33, 424 (1974).
- ⁸J. J. Rhyne (unpublished).
- ⁹K. H. J. Buschow and R. P. Von Stapele, *J. Appl. Phys.* 41, 4066 (1970); and L. J. Tao, S. Kirkpatrick, R. J. Gambino, and J. J. Cuomo, *Solid State Commun.* 13, 1491 (1973).
- ¹⁰S. Kobe and K. Handrich, *Phys. Status Solidi* 54, 663 (1972).
- ¹¹E. Burzo, *Zeit. fur Angew. Phys.* 32, 127 (1971).
- ¹²First observed in high-field measurements by A. E. Clark, *Appl. Phys. Lett.* 23, 642 (1973).
- ¹³L. Néel, *C. R. Acad. Sci. (Paris)* 228, 664 (1949); also see S. Chikazume, *Physics of Magnetism* (Wiley, New York, 1966), p. 314.
- ¹⁴K. W. H. Stevens, *Proc. Phys. Soc. Lond. A* 65, 209 (1952).
- ¹⁵L. J. Tao, S. Kirkpatrick, R. J. Gambino, and J. J. Cuomo, *Bull. Am. Phys. Soc. Ser. II* 19, 207 (1964), and private communication.
- ¹⁶J. Orehotsky and K. Schröder, *J. Appl. Phys.* 43, 2413 (1972).